Astron. Astrophys. 148, 243–253 (1985)

ASTRONOMY AND ASTROPHYSICS

The large and small scale radio structure of 3C236

P. D. Barthel[1,*], R. T. Schilizzi[2], G. K. Miley[1,], W. J. Jägers[1], and R. G. Strom[2]**

[1] Leiden Observatory, P. O. Box 9513, NL-2300 RA Leiden, The Netherlands
[2] Netherlands Foundation for Radio Astronomy, P. O. Box 2, NL-7990 AA Dwingeloo, The Netherlands

Received December 12, 1984; accepted February 4, 1985

Summary. The radio emission of the largest known object in the universe, the radio galaxy 3C236, has been studied in detail with resolutions of 23 arcsec to 1 milliarcsec. The 40 arcmin overall structure has been observed with 4000:1 dynamic range using the Westerbork array, and the subarcsecond nuclear structure has been mapped with transatlantic VLBI arrays, in combination with MERLIN. Striking similarities between the large and small scale structures are found. Assuming a physical origin for these similarities, we argue that a long-lasting asymmetric interaction of the energy flow with the core environment is responsible for the overall morphology in 3C236. The evolution of the radio galaxy is also discussed and a scenario-dependent age of $10^{9\pm1}$ yr is proposed.

Key words: galaxies – radio observations – active galaxies – VLBI

1. Introduction

The radio galaxy 3C236 is of considerable astrophysical interest. Its radio structure constitutes the largest known object in the universe (~ 4 Mpc – using $H_0 = 75$ km s^{-1} Mpc^{-1}) and contains a bright steep-spectrum core of about 2 kpc overall size. This large range in scale size suggests that we are simultaneously observing both relatively young and relatively old radio emission in this source and that comparison of the morphology of the steep-spectrum radio structure in the core with the overall morphology of the source may give important information on the evolution of extended radio sources, and on the mechanisms of radio source formation in general. We report here on three sets of measurements which delineate the nuclear structure in relation to the large scale overall structure in 3C236:

(i) Observations with the 3 km Westerbork Synthesis Radio Telescope (WSRT) in its redundant configuration at 1.4 GHz to obtain a dynamic range of more than 35 dB at about 15″ (25 kpc) resolution, (ii) eight – station transatlantic VLBI observations combined with five-station MERLIN data at 1.6 GHz, to give a relatively uniform spatial frequency coverage and resolution of 25 milliarcsec (43 pc) for the $\sim 1''$ nuclear structure, and (iii) four-station transatlantic VLBI observations at 5 GHz to obtain about 1.5 milliarcsec (2.5 pc) resolution.

Send offprint requests to: P. D. Barthel
* Present address: Caltech 105-24, Pasadena CA 91125, USA
** Present address: Space Telescope Science Institute, Homewood Campus, Baltimore MD 21218, USA

The structure of the paper is as follows. In Sect. 2 we review earlier observations, in order to set the scene for the present work on 3C236. Our observational procedures will be described in Sect. 3, and the various results will be presented in Sect. 4. These results contain information on completely different size scales, and in Sect. 5.1 of the Discussion attention will be drawn to several striking similarities in the large and small scale radio structure. Sections 5.2–5.4 are concerned with the implications of our results for the formation, evolution and age of the radio galaxy.

2. The source structure so far

The giant radio source 3C236 has a narrow double morphology, with an overall angular size of 40′ (Willis et al., 1974; Strom and Willis, 1980, S&W hereafter), and is identified (Wyndham, 1966) with an elliptical galaxy at redshift $z = 0.0988$ (Sandage, 1967). At this redshift the total linear size of the source is 4 Mpc; 3C236 is the largest radio source known.

The dominant compact radio core of 3C236 has a steep radio spectrum ($\alpha = -0.7$, $S_\nu \propto \nu^\alpha$) and has been the subject of several studies. Single-baseline interferometric observations by Wilkinson (1972) showed that the radio core could be modelled by a 1″ double in position angle 119°. Fomalont and Miley (1975) confirmed and refined this model with a higher resolution interferometric study. Moreover, they were able to show that the radio core structure represents a relatively recent event in the nucleus of 3C236, implying directional stability over at least $10^{7.5}$ yr. They also deduced that off-axis fine structure existed in the core, and drew attention to some similarities between the structure of the core and that of the overall source.

From 1975 onwards, several VLBI experiments studying the radio core of 3C236 were carried out (Preuss et al., 1977; Schilizzi et al., 1979, 1981). At λ 18 cm Schilizzi et al. (1981) showed that the south eastern component of the double was composed of a triple structure with separations of 120 and 340 pc, well aligned with the position angle of the large scale structure. The components were labelled A, B 1, B 2 and C (west to east), of which B 1 and B 2 were unresolved at ~ 40 mas resolution. They were regarded as the best candidates for the true radio nucleus of 3C236.

Meanwhile, the core was also the subject of some high resolution observations with the Very Large Array in order to study spectral and polarization characteristics of the radio morphology (Fomalont et al., 1979, 1982). The maps, at 2.7, 5, 15, and 22.5 GHz, are in good agreement with the VLBI observations, and the (B 1 + B 2) complex is found to be opaque at high frequencies: $S_\nu \propto \nu^{0.15}$.

3. Observational procedures

3.1. 1412 MHz WRST observations

We observed 3C236 with the 3 km 14 antenna Westerbork Synthesis Radio Telescope (WSRT) in two observing sessions of 12 h each (36 m and 72 m were the shortest spacings), during the latter half of 1982. The observing frequency was 1412 MHz (21.2 cm wavelength) with a bandwidth of 10 MHz. In order to map the low surface brightness lobe emission as reliably as possible, we used the redundancy mode of the WSRT (Noordam and De Bruyn, 1982). In this mode, optimum use is made of the large number of redundant interferometer spacings that are present in the array to suppress gain and phase errors, thereby improving the dynamic range. The "optimized" data were Fourier transformed and the resulting map was cleaned using standard algorithms.

3.2. 1.6 GHz VLBI and MERLIN observations

18 cm VLBI observations of the nucleus of 3C236 [$\alpha(1950 = 10^h03^m05^s.40$, $\delta(1950) = 35°08'47''.7$] were made with an eight station global network on 12 October 1982, using standard MkIIC equipment (Clark, 1973). Table 1 gives the relevant telescope parameters. The observing frequency was 1660 MHz, the polarization LCP. Correlation of the data was carried out on the CIT/JPL correlator at the California Institute of Technology, Pasadena, USA. The correlation coefficients were integrated for 2 min and calibrated following the precepts outlined by Cohen et al. (1975). Consistency checks on closure phase and closure amplitude were made separately for the European and US subsets of telescopes using 0235+164, *OQ*208 and DA 193.

An important addition to the $u-v$ coverage was made by adding five-station MERLIN (Davies et al., 1980) data at 1660 MHz to the data set. The epoch of observation was 20 August 1980, and the $u-v$ data were made available by Dr. T. J. Cornwell. The fringe amplitudes of the MERLIN data were reduced by 8% to force agreement between the maximum visibility on the shortest baseline and the total flux density in the nucleus (2.86 Jy) obtained from interpolation of the spectrum given by Fomalont et al. (1979). In combining the VLBI and MERLIN data sets we have assumed that the structure did not vary between the epochs of observation, and that the small scaling errors caused by combination of data at slightly different frequencies will not be troublesome. We used the self-calibration mapping algorithms in both the CIT/VLBI and AIPS packages, en route to the final radio map.

Table 1. Parameters of the interferometer array, at λ 18 cm

Telescope location	Diameter (m)	T_{sys}(K)	Antenna sensitivity (K/Jy)
Effelsberg, FRG	100	50	1.45
Dwingeloo, NL	25	37	0.11
Jodrell Bank, UK	76	60	1.00
Onsala, Sweden	26	27	0.09
Haystack, USA	37	120	0.075
Green Bank, USA	43	50	0.25
Socorro, USA	130	60	1.50
Owens Valley, USA	40	85	0.20

Table 2. Parameters of the interferometer array, at λ 6 cm

Telescope location	Diameter (m)	T_{sys}(K)	Antenna sensitivity (K/Jy)
Effelsberg, FRG	100	78	1.60
Green Bank, USA	43	66	0.27
Socorro, USA	130	60	2.3
Owens Valley, USA	40	133	0.23

3.3. 5 GHz VLBI observations

We observed the radio core of 3C236 with a four station transatlantic VLBI network for 16 h on April 9/10, 1981, using the standard MkIIC equipment (Clark, 1973). Table 2 gives the relevant telescope parameters. The observing frequency was 4990 MHz, the polarization LCP. The lobe spacings for the interferometers range from about 20 to 1.5 milliarcsec. Correlation of the data was carried out at the Max-Planck-Institut für Radioastronomie, Bonn, FRG. After determining coherence losses we integrated the correlation coefficients for 6 min, and calibrated them according to Cohen et al. (1975), using 0235+164 as calibration source. The hybrid mapping technique developed by Cornwell and Wilkinson (1981) yielded the final radio map.

4. Results

In this section we show the maps obtained in the observations described above. Physical source (component) parameters derived from the various observations using standard assumptions, are listed in Table 3 at the end of this section.

4.1. 1412 MHz WSRT

The final map, after restoration with a $13'' \times 23''$ beam is reproduced in Fig. 1, and the lobes are shown in more detail in Figs. 2 and 3. These figures show the radiation of the combined Stokes parameters ($I-Q$), which is the single quantity measured by the WSRT in its redundancy mode. The point source in the nucleus of 3C236 has a 1412 MHz flux density of 3310 ± 30 mJy, and the noise level in the maps is $\lesssim 0.8$ mJy per beam: the dynamic range obtained is about 4100:1.

Note that the highest contour level (excluding point sources) in Figs. 2 and 3 corresponds to 0.2 and 0.6%, respectively of the peak brightness in the field. Comparison with previous 21 cm WSRT maps of 3C236 (S&W) clearly shows the effects of higher resolution (3 km vs. 1.5 km array), smaller beam area, and higher dynamic range.

The most notable results of our new observations are:

4.1.1. The megaparsec – scale gaps

Inspection of Fig. 1 shows that there is no detectable radio emission, to a level of 0.5 mJy per beam ($\sim 10^{22}$ WHz^{-1}) within about 6′ (600 kpc) of the associated giant elliptical galaxy to the NW, and within about 18′ (1.8 Mpc) to the SE.

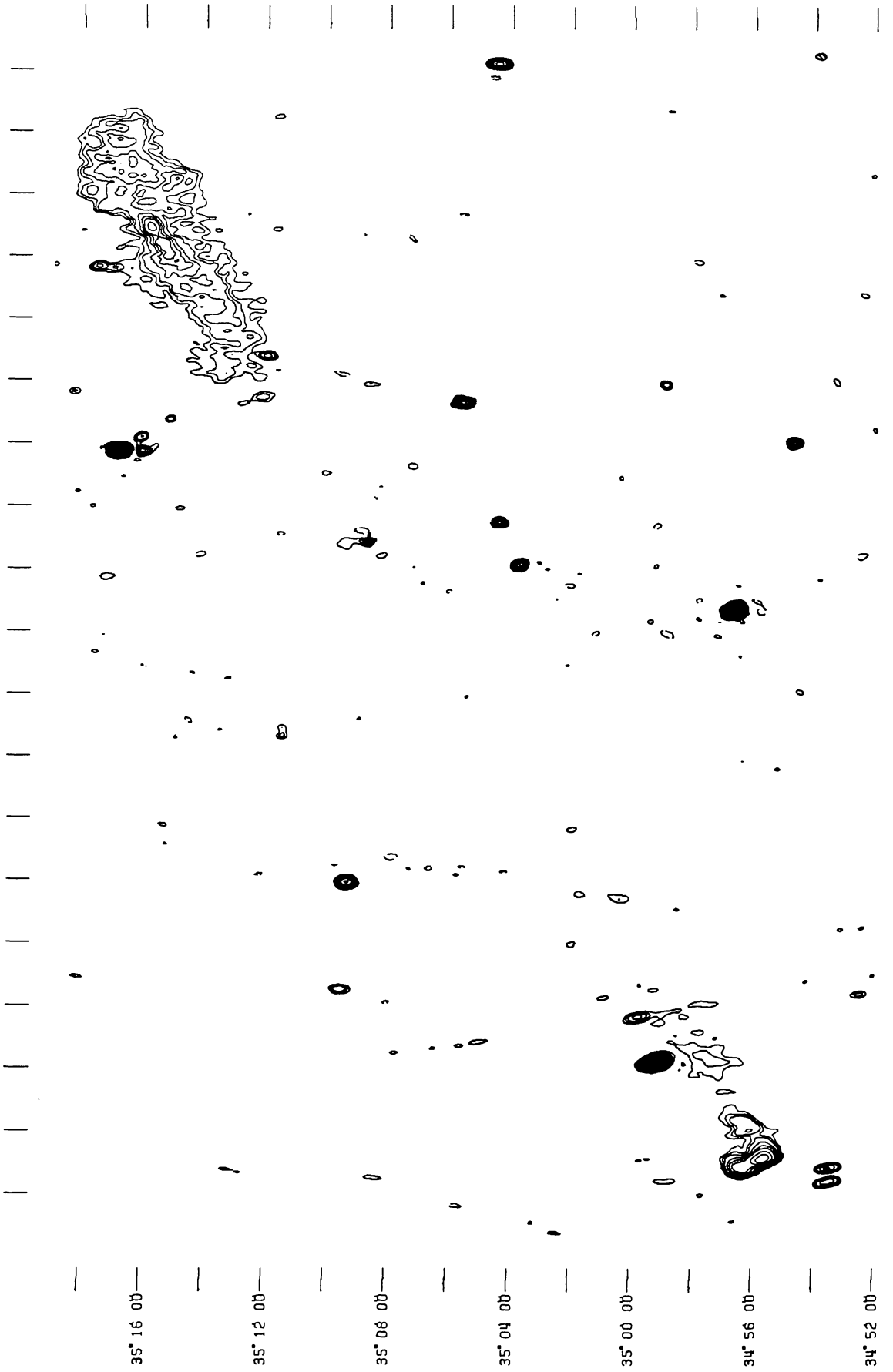

Fig. 1. 3C236 at 1.4 GHz; restoring beam is $13'' \times 23''$, and is shown in lower right corner; contour levels are $-1, 1, 1.5, 2, 3, 4, 5, 7, 9, 11, 13, 15, 19, 23, 27, 31, 35, 43, 51, 59, 67, 75, 91, 107, 123, 139, 155, 187, 219, 251, 283, 315$ mJy/beam; the point source in the nucleus, at the position of the + sign, has been removed

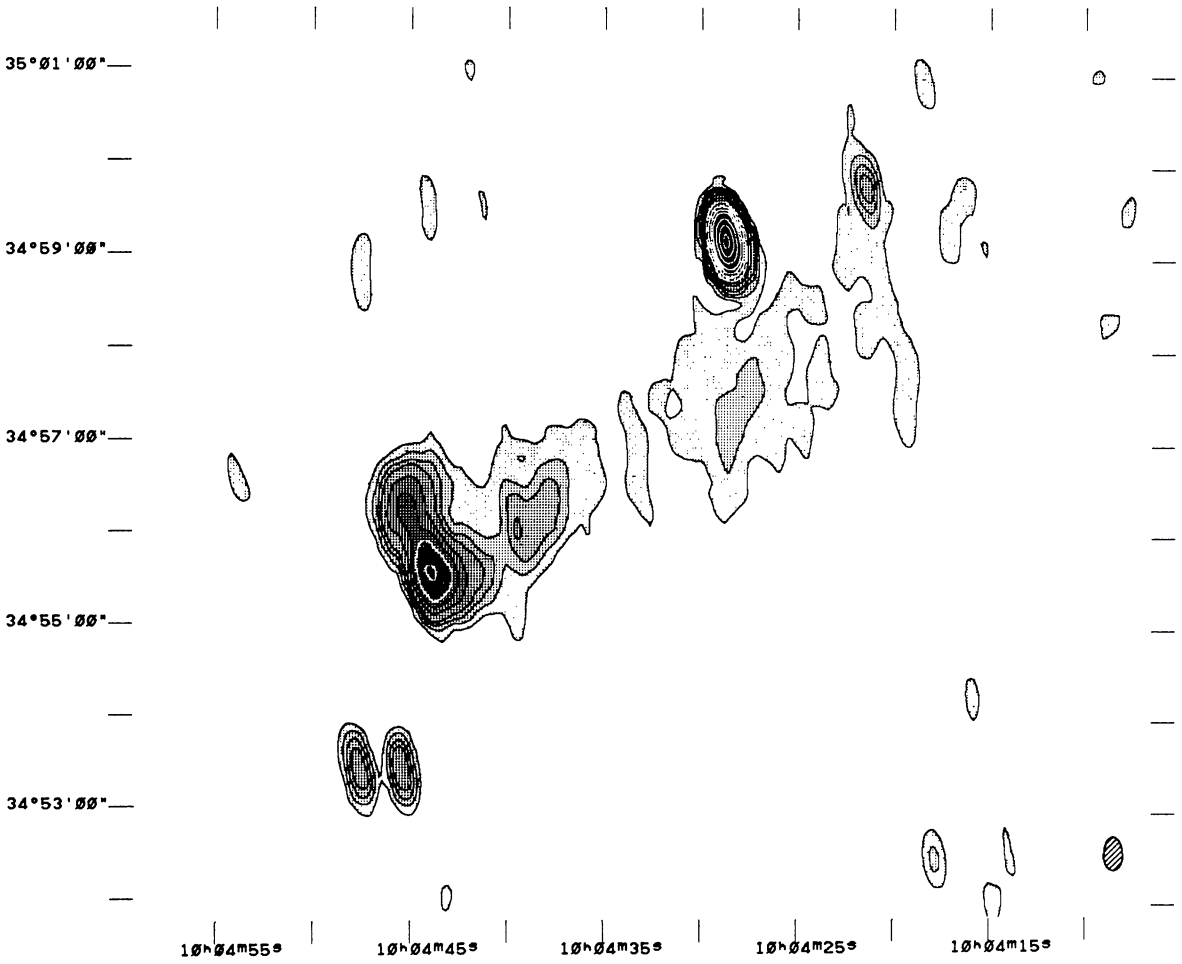

Fig. 2. 3C236 SE lobe in more detail; contour levels are 0.75, 1.5, 2.25, 3.0, 3.75, 4.5, 5.25, 6.0, 6.75, 7.5, 9 mJy/beam; restoring beam as in Fig. 1

4.1.2. The SF (double) hot spot

The SE lobe (Fig. 2) extends about 600 kpc and has a double hot spot at its leading edge, which is about 2.5 Mpc from the galaxy. The trailing radio emission towards the galaxy has a somewhat curved trajectory and low surface brightness of about 1–3 mJy per synthesized beam ($13'' \times 23''$ FWHM). We find no significant trailing emission from the secondary (northern) hot spot towards the galaxy, apart from a weak grating ring response. According to S&W, the primary hot spot is found to be strongly polarized ($P/I = 57 \pm 10\%$) at 5 GHz with the magnetic field in p.a. $16° \pm 4°$, i.e., directed towards the secondary hot spot. Faraday rotation at 5 GHz will have a negligible effect on the derived position angle.

4.1.3. The wiggles in the NW lobe

The NW lobe (Fig. 3) with overall linear size of about 1 Mpc does not show a compact hot spot at its leading edge, but rather a broad relaxed plateau. This plateau lies at a distance of about 1.5 Mpc from the associated galaxy. A dominant inner ridge is visible, which does show a pronounced compact hot spot. The diffuse trailing radio emission has a low surface brightness of a few mJy per synthesized beam. A large scale wiggle can be seen in the NW lobe. Careful inspection of the previous 21 cm and 50 cm maps (S&W) reveals the same effect. In order to represent this large-scale wiggle as well as possible we show rotated and slightly convolved maps of the lope structures in Fig. 4, indicating the wiggle by broken lines.

The inner ridge in the NW lobe is probably a much younger event in the history of 3C236 (see following) with its emission superimposed on the lower brightness radio emission. By plotting only low level contours in Fig. 4 we have restricted ourselves to the low brightness emission. The wavelength of the wiggle is about 300 kpc. The same wiggle may be present in the SE lobe (see Fig. 4). We finally note that the inner ridge in the NW lobe also shows curvature (see Fig. 3).

4.1.4. Background sources

Many background sources are seen in the vast 3C236 field. The radio source south of the SE hot spot is resolved into a 28″ double in p.a. 83°; it has no optical identification (S&W – their background source E). Near the NW lobe two unresolved features are seen, labeled *A* and *F*. "*A*" has been discussed by S&W, who did not find an optical counterpart for this (assumed) background source. The same authors did not resolve component *F* for which we measure a (1950) position RA $10^h02^m36\overset{s}{.}0$, Dec 35°12′05″; we have identified *F* with an 18^m–19^m galaxy on the Palomar Sky Survey E plate.

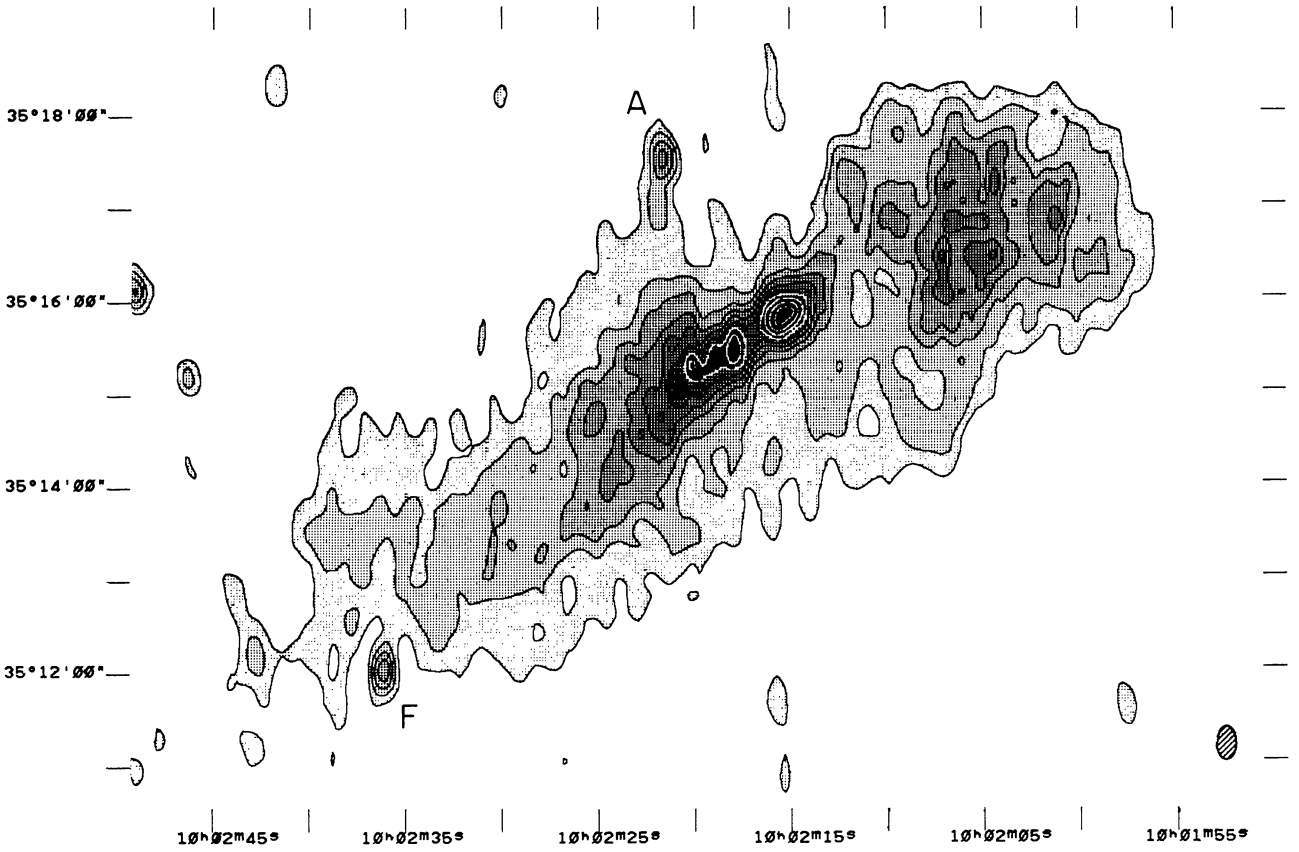

Fig. 3. 3C236 NW lobe in more detail; contour levels are 0.75, 1.5, 2.25, 3.0, 4.5, 6.0, 7.5, 10.5, 13.5, 16.5, 22.5, 28.5 mJy/beam; restoring beam as in Fig. 1; two background sources are indicated (see text)

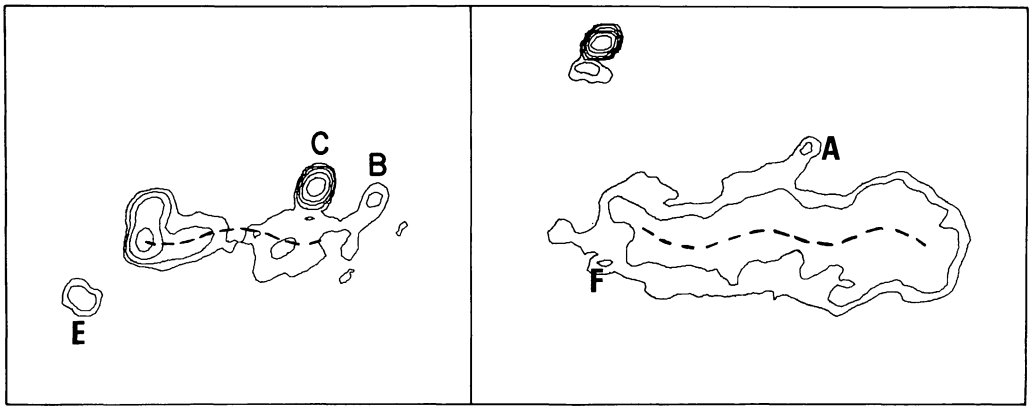

Fig. 4. 3C236 low level lobe emission; source has been rotated and smoothed with a beam five times greater than the original in horizontal direction; contour levels are 0.75, 1.5, 3, 6, 12, 24 mJy/beam; five background sources are indicated

4.2. 1.6 GHz VLBI & MERLIN

The final map, after restoration with a 24×25 mas beam in p. a. 90°, is shown in Fig. 5. In obtaining that map we restricted the $u-v$ coverage to a maximum spatial frequency of $15\,M\lambda$ to ensure a relatively uniform and circular coverage for this complicated structure. Even so, the fit to the shortest VLBI baseline is not perfect, indicating difficulties in recovering the broad structure in the West with a 25 mas beam. When no restriction was placed on the $u-v$ coverage, it was not possible to obtain a good fit to the data, presumably because the $u-v$ coverage is too patchy at large spatial frequencies to allow a proper recovery of a structure that is about 80 beams long and 35 beams wide. The various components already mentioned in Sect. 2 are indicated.

The most striking features of these observations are:

4.2.1. The (B 1 + B 2) core complex

Component B 2 is the most compact component in the 2 kpc radio core, since B 1 shows resolution effects. A halo of low surface brightness emission is centered on B 2.

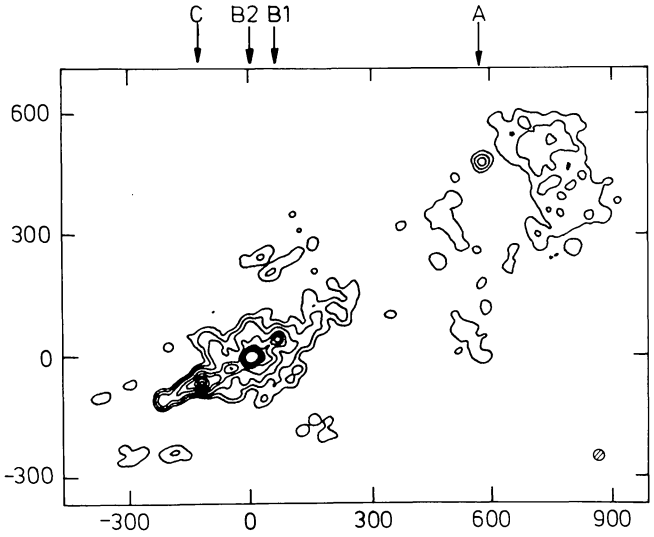

Fig. 5. 3C236 core at 1.67 GHz; restoring beam is 25 milliarcsec, and is shown in lower right corner; contour levels are 1, 2.5, 5, 10, 15, 20, 25, 30, 35, 40, 45% of peak brightness, which is 277 mJy/beam; scale is in milliarcsec

4.2.2. The jetlike structure to the east

Component *C* (actually a chain of components), eastward from B 2 appears to be a 250 mas (~400 pc) jet, which oscillates about a direction which is some 10° different from the overall source elongation.[1] Going eastward in *C* there is a sudden brightening, inmediately followed by a change in position angle. At that point, the jet passes through a transverse structure, as is evident from a higher-resolution map (excluding the MERLIN data). This argues for identification with an internal, oblique shock, giving rise to particle acceleration and/or magnetic field amplification as well as beam deflection (compare Rees, 1979). The structure resembles the jet structure in M 87, albeit on smaller scale (Owen et al., 1980; Biretta et al., 1983).

4.2.3. The diffuse structure to the west

About 1.5 kpc westward from B 2 an extended low surface brightness region is found, the peak of which has been labeled *A* in earlier work. This peak *A* is located definitely north of the source axis, in p. a. −50°. Famalont et al. (1982), reported that *A* is the peak of a broad relaxed component with a fairly high thermal matter density and steep radio spectrum ($S_\nu \propto \nu^{-0.75}$). The nature of *A* is unclear, but it could be the remnant of an earlier shock deflection as in component *C*.

4.3. 5 GHz VLBI

The final map, restored with a 2.3 × 1.0 mas beam (p. a. 140°), is shown in Fig. 6.

Due to station failure during the observations pronounced gaps arose in the aperture plane coverage which have resulted in a fairly high sidelobe level. From examination of the residual noise level, we are confident about the correctness of this map to the fifteen percent level.

1 The overall p. a. of 3C236 is taken to be 122°5 (−57°5), as determined from the 610 MHz observations (Willis et al., 1974)

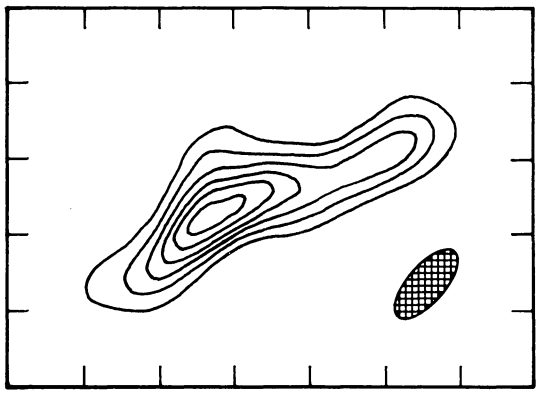

Fig. 6. 3C236 core at 5 GHz; restoring beam is 2.3 × 1.0 milliarcsec in p.a. 140°, and is shown in lower right corner; contour levels are 15, 30, 45, 60, 75, 90% of peak brightness, which is 84 mJy/beam; tick interval is 2 milliarcsec

In addition to the 320 ± 30 mJy component shown, we also detected (on the short VLA-OVRO baseline) a 50 ± 10 mJy component at 75 mas in p. a. −58°. We identify the former with B 2 and the latter with B 1 (compare Fig. 5).

A composite map of the large and small radio morphology in 3C236 is finally shown in Fig. 7. The following conclusion can then be drawn from these observations.

4.3.1. Identification of the "true" nucleus

Several arguments strongly suggest that component B 2 should be identified with the actual nucleus in 3C236: (i) in both 6 and 18 cm VLBI observations, component B 1 shows resolution effects; B 2 however is unresolved on the 18 cm map; (ii) combining the 5 GHz total flux density and the 1.6 GHz peak flux density in B 2 we obtain a flat or slightly inverted radio spectrum for this component; since the (B 1 + B 2) complex was found to be opaque at high frequencies (Sect. 2), the (resolved) B 1 component must have a steep radio spectrum; (iii) a halo of low surface brightness emission is centered on B 2, as deduced from the 1.6 GHz observations (Sect. 4.2.1).

Having identified B 2 with the true nucleus we note with particular interest that the kpc radio structure in the core of 3C236 is highly asymmetric with respect to its actual center, both in length and in morphology.

4.3.2. Morphology of the nucleus

Although asymmetric with its main extension to the west, the B 2 component is two-sided. Its overall angular size of 10 mas converts to a linear size of about 16 parsec.

4.3.3. Orientation of the nucleus

The main axis defined by B 2 (from its peak to the west) has p. a. 110°, which is 12° different from the overall p. a. of 3C236 – see previous footnote. This offset had been suggested earlier by Schilizzi et al. (1981) from lower resolution observations.

4.4. Source and source component parameters

Table 3 lists some measured and derived parameters for the various components of 3C236. In the calculations the radio window has been taken from 10^7–10^{10} Hz, and we assumed cylindrical geometry, unity filling factor, energy equipartition and random pitch angle distribution.

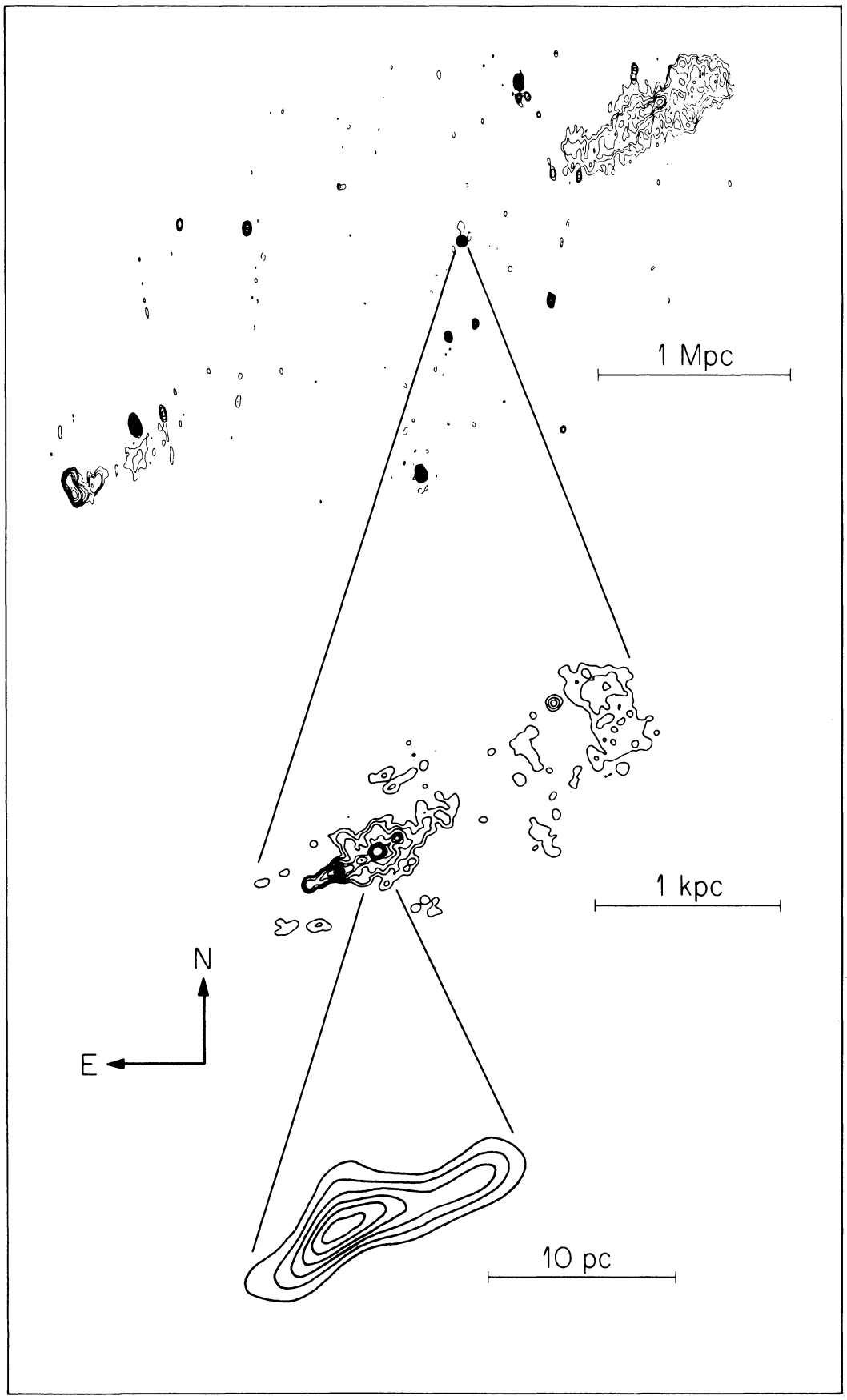

Fig. 7. Composite map showing the radio morphology of 3C236; linear scales are indicated

Table 3.

The large scale structure

Component	P_{21} (W Hz^{-1})	L_{radio} (erg s^{-1})	P_{min} (dyne cm^{-2})
NW lobe	$2\,10^{25}$	$2\,10^{42}$	$6\,10^{-13}$
SE lobe	$1\,10^{25}$	$1\,10^{42}$	$6\,10^{-13}$
Core	$6\,10^{25}$	10^{42}	see below

The small scale nuclear structure

Component	Size (cm^3)	L_{radio} (erg s^{-1})	P_{min} (dyne cm^{-2})
B 1	10^{58}	10^{40}	10^{-6}
B 2 core	$\lesssim 10^{55}$	10^{40}	$\gtrsim 10^{-5}$
B 2 jet	10^{56}	10^{41}	10^{-5}
C	10^{60}	10^{41}	10^{-7}

5. Discussion

The discussion will concentrate on the implications of the currently available observational material. The large amount of data enables us to study the relation between the large and the small scale radio structure in 3C236. In Sect. 5.1 we draw attention to striking similarities between the large and small scale structure and assuming a physical origin for these similarities we argue, in Sect. 5.2 and 5.3 that a long-lasting asymmetric interaction of the energy flow with the core environment is responsible for the overall structure of 3C236. Finally, Sect. 5.4 is concerned with the age of the radio galaxy.

5.1. Similarities in the large and small scale morphologies

Identifying component B 2 with the actual nucleus in 3C236, several striking similarities are seen between the morphologies of the megaparsec-scale structure (Fig. 1) and the kpc-scale core (Fig. 5):

5.1.1. Asymmetric extensions

The 2 kpc radio structure in the core is not of equal length east and west of the actual center: the extension to the west is about three times longer than that to the east. The 4 Mpc overall radio structure in 3C236 is similarly asymmetric, but in the other direction; here the extension to the west is about one and a half times smaller than the eastern one.

5.1.2. Asymmetric collimation

Core and overall structure are also asymmetric in morphology. The core structure is jetlike to the east and diffuse to the west. Regarding the overall radio structure a prominent leading hot spot is found in the SE lobe, whereas such a hot spot is not present in the NW lobe. Seen from B 2 the various large and small scale emission regions define opening angles which are larger to the west than to the east, but similar for the small and large scale structures.

The angle subtended by the SE lobe is $\sim 4°$, by the nuclear jet C $\sim 6°$ (deconvolved with the VLBI beam). We also note that both angles are offset to the north from the overall source p. a. (122°.5). The angle subtended by the NW lobe is $\sim 14°$, symmetrically with respect to the overall source axis. Although difficult to determine, the angles subtended by the diffuse western core emission is about 18°, again symmetrically with respect to the overall source axis. This opening angle asymmetry from east to west had been noted previously by Fomalont and Miley (1975), from much less detailed data.

5.1.3. Wiggles and off-axis structure

In Sect. 4.1.3 we have seen that the large scale structure exhibits wiggles on a scale of about 300 kpc. From Sect. 4.2.2 the nuclear jet (component C) also has a structure which is off axis and shows bends on a scale of about 100 pc. Finally, the 10 pc western extension in the nucleus B 2 (Fig. 6) defines a direction which is some 10° different to the overall source axis. All these offsets are in rough agreement with the above mentioned large scale opening angles.

5.2. Interpretation of wiggles and off-axis structure

In Sect. 5.1 we drew attention to the existence of off-axis, bending or wiggling structure in both the large scale emission and the small scale nucleus. It is possible that this similarity is coincidental, but it is intriguing enough to warrant consideration of possible common origins for the wiggles in some detail.

Interpreting the latter as being left behind by a beam advancing with a velocity of about $0.1c$ (Sect. 5.4) the wavelength of the large scale (300 kpc) and small scale wiggle (0.1 kpc) implies a period of the order of 10^7 yr and 10^3 yr respectively.

Possible explanations for wiggles in radio sources include (see e.g., Trussoni et al., 1983): 1. orbital motion around a companion galaxy; 2. fluid dynamical bending; and 3. a precessing beam. These possibilities will be commented on separately, although more of them can simultaneously explain the large and small scale wiggles.

5.2.1. Orbital motion

Jet curvature caused by gravitational interaction (Blandford and Icke, 1978) implies low flow speeds ($\sim 10^2$–10^3 km s^{-1}), which seems to be in contradiction with the observations (see following), and furthermore would imply an age for 3C236 in excess of 10^{10} yr. Besides, no neighbour galaxies are seen (S&W).

5.2.2. Hydrodynamic instabilities

Fluid-dynamical twisting, caused by helical Kelvin-Helmholtz instability modes with long wavelengths, can be characterized in the linear regime and for high Mach numbers by

$$\lambda_h/R = M(a + b \ln \bar{\varrho})$$

(Ferrari et al., 1983), where λ_h is the helical mode wavelength, R the flow radius, M the flow Mach number and $\bar{\varrho}$ the density ratio of material inside and outside the jet ($=\varrho_{\rm flow}/\varrho_{\rm igm}$). The constants a and b are listed by Ferrari et al. (1983), and using $R \lesssim 3$ kpc (radius of the hot spot in SE lobe) we obtain for an MHD flow:

$$\ln \bar{\varrho} \lesssim 6.5\text{–}500/M\,.$$

This would indicate that all jets except those with $M \gtrsim 10^2$ should be extremely light. However, neither $\bar{\varrho}$ nor M is known so the model of fluid dynamical twisting cannot be tested properly here. The occurence of such flow instabilities might nevertheless disrupt the efficient energy flow, give rise to particle acceleration and make the flow visible.

5.2.3. Wobbling of ejection axis

Another possible explanation for wiggles is wobbling or precession of the ejection axis in the nucleus of the active galaxy. Begelman et al. (1980) have shown that in a massive black hole binary, the spin axis of the more massive hole may precess about the total angular momentum of the binary with a period.

$$P_{\rm prec} \sim 600 r_{16}^{5/2} (M/m) M_8^{-3/2}\ {\rm yr}\,,$$

where r_{16} is the binary separation in units of 10^{16} cm, M_8 the mass of the larger hole in units of $10^8 M_\odot$, and M/m the mass ratio. For $r_{16} \sim 25$, $M/m \sim 10$ and $M_8 \sim 1$ a precession period of the order of the one inferred for the large scale structure will result. The off-axis bends of the nuclear jet might then be the result of a powerful interaction between the radio jets and the dense, inner galactic environment (see Sect. 5.3).

5.3. *Production of observed radiation*

One of the most topical questions in radio astrophysics at present concerns the relation of the observed emission in extended radio sources to the energy transported by jets from their nuclei. How is the energy converted to radio emission and do invisible jets exist? Our 3C236 results contain information which is relevant to this problem. We need to account for the exceptionally bright nucleus, for the Mpc gaps between the nuclear structure and the outer lobes, and for the asymmetry in appearance, and distance from the nucleus of the two outer lobes.

There are three general mechanisms which may bear on the strength of the nucleus: relativistic beaming, accumulation of plasmons ejected from the nucleus, and interaction of a beam with the interstellar medium in the nucleus. The high surface brightness in isolated compact radio sources and the apparent asymmetry in (nuclear) jets in otherwise symmetric extended extragalactic radio sources has been explained as being caused by relativistic beaming close to the line of sight (Blandford and Königl, 1979; Readhead 1980). The discovery of very extended structures surrounding the superluminal sources by Schilizzi and De Bruyn (1983) prompted the suggestion that the axis of the emission in these sources has precessed from near the plane of the sky into the line of sight. That this could be the case in 3C236 seems unlikely for the following reasons: (i) the nuclear structure appears two-sided even on scales of a few milliarcsec, which could not be so if Doppler boosting was important; (ii) as Saikia (1981) has pointed out, highly relativistic velocities ($v/c > 0.9$) are not compatible with the observed relationship between spectral index and luminosity for steep spectrum nuclei in extended extragalactic radio galaxies ($\alpha - P$ relationship; see Bridle and Fomalont, 1978; Fomalont et al., 1980), a relationship satisfied by 3C236; (iii) the inner-outer alignment is quite good, which is unlikely if the axis has changed direction substantially.

We contend that the high core brightness and the asymmetric nuclear structure reported here for 3C236 argue strongly for intrinsically bright and intrinsically asymmetric emission in the core, since the source (a) satisfies the $\alpha - P$ relationship, and (b) very probably lies in the plane of the sky, because its projected linear size is already very large. By inference, high core brightness without relativistic beaming, and intrinsic asymmetry could also occur in other sources.

The high core brightness could be generated by emission in the form of independent plasmons. The idea that 3C236 is powered and has been built up by subsequent ejection of (numerous) plasmons from its core was proposed by S&W (1980). This idea was partly based on their observation of the inner ridge in the NW lobe, the lower-resolution observation of a simple double morphology in the core (Fomalont and Miley, 1975), and subsequent identification of these components with independent plasmons. However, the present observations, described in Sect. 3 have revealed a more complicated nuclear structure, making this scenario less likely. Also the origin of the large scale wiggles in the lobes is difficult to envisage in this scenario. Moreover, we regard the age of $\gtrsim 10^{11}$ yr deduced by S&W on the basis of their model as improbably large (see Sect. 5.4). We therefore prefer the third mechanism, that the high core brightness could be due to inefficiency in the energy flow in the inner part of the associated galaxy.

Regarding this possibility, it is appropriate to stress that a radio feature locates a place of lossy energy transport and not necessarily more than that. The features A, B 1, and C need not preferentially be identified with independent plasmons being ejected by the core B 2. There are several facts supporting the idea that the core emission in 3C236 indeed arises from an interaction between the energy flow and the hot and dense inner galactic environment. First, the size of the 3C236 radio core is roughly the same as that of a typical optical narrow (emission) line region (NLR) (e.g., Osterbrock, 1984). Second, there is no detectable radio emission (to the level of 0.5 mJy/beam, corresponding to $10^{22}\,{\rm WHz}^{-1}$), in the region between ~ 1 kpc and many hundreds of kpc from the core. Third, for active galaxies the [O III] line widths are correlated with the luminosities of associated kiloparsec-scale radio emission, indicating that the forbidden line region plays an important role in the production of this radio emission (Heckman et al., 1981). For 3C236 the [O III] line width ($1000\,{\rm km\,s}^{-1}$ FWHM, Miley and Osterbrock, 1979) is extremely wide, consistent with the observed bright kiloparsec radio emission. Fourth, from depolarization a thermal density of $\sim 3\,10^{-3}\,{\rm cm}^{-3}$ in component A is derived (Fomalont et al., 1982), which is unusually high, and suggests that a relatively dense thermal medium coexists with the radio emission. Fifth, the minimum pressure in the core components (see Table 3) exceeds typical NLR parameters ($n_e \sim 10^{3-4}\,{\rm cm}^{-3}$, $T \sim 10^4$ K). Sixth, with a size of 2 kpc and radio spectral index of 0.7, the core satisfies the definition of an SSC (Steep Spectrum Core), as recently discussed

by Van Breugel et al. (1984). There is considerable evidence (see Van Breugel et al., 1984 and references therein for the various arguments) that such SSC's are being produced by the interaction of an outward moving beam with the optical NLR. Before discussing this interaction in more detail, we draw attention to the fact that most of the core emission in 3C236 originates from off-axis regions and components. Although speculative, this may even indicate that the brightness of the core in 3C236 (and other steep-spectrum-core radio galaxies?) is caused by the interaction with the inner galactic environment of off-axis (precessing?) beams in an extended radio source with an otherwise well-defined axis. We also note that the core in 3C236, although bright, does not contain an excessive amount of energy: $E_{\min} \sim 10^{55}$ erg, compared to $\sim 10^{59}$ erg for the radio lobes.

Adopting the scenario that the high core brightness in 3C236 is indeed produced by violent interactions with hot and dense gas in the NLR, two conclusions can be drawn from our data. First, the apparent asymmetry, both in extension and in collimation in the core would indicate asymmetric interaction with respect to the actual nucleus B 2. Although this asymmetry is defined in a region having a radius of about 1 kpc, the interaction radius to the SE appears to be three times shorter than that to the NW. Second, not only the core but also the large scale structure in 3C236 is asymmetric in extension and morphology. This large scale asymmetry could be a natural consequence of the asymmetric interaction in the core: the eastern, well collimated jet in the core would give rise to the compact SE hot spot, whereas the diffuse, badly collimated core emission to the west would explain the diffuse NW lobe. The well collimated outflow to the south-east might also explain the fact that the SE lobe extends a megaparsec further in the IGM than the NW lobe. On the assumption then, that asymmetric core interaction is indeed the physical origin for the overall asymmetric appearance of 3C236, this interaction must be long-lasting. A lower limit to the relevant time scale is of course the light travel time to the SE hot spot, which is $10^{6.9}$ yr. With a more probable hot spot advance velocity the time scale over which asymmetric interaction must take place would be an order of magnitude larger.

Trying to explain this intriguing property of the long-lasting asymmetric core interaction would be premature since not much is known about morphology and spectral properties in, particulary, the optical domain.

Finally we draw attention to the peculiar emission at the leading edge of the SE radio lobe. The SE lobe was already discussed in Sect. 4.1 where attention was drawn to the presence of a double hot spot at the leading edge of the lobe, the curved trailing emission, and the magnetic field structure in the double hot spot. The equipartition magnetic field strength in the diffuse lobe emission is about 1 μG. Thermal pressure balance of the relativistic lobe plasma is therefore likely, as this requires

$$B_{eq} \sim 10^{-6} \left(\frac{n}{10^{-5}} \frac{T}{10^{7}} \right)^{1/2} \text{Gauss},$$

with values $n \sim 10^{-5}$ cm and $T \sim 10^{7}$ K being normally found in the IGM (Begelman et al., 1984). The primary hot spot might be identified as the place where particle acceleration and magnetic field amplification are taking place. Deflection of the beam can be produced by an oblique shock in the beam generated by a non-axisymmetric disturbance on its working surface. The morphology as well as the magnetic field structure suggests that this is taking place in the SE lobe of 3C236 (see also Lonsdale and Barthel, 1985). (Partial) ram pressure balance of the deflecting working surface is possible as this requires

$$B_{eq} \sim 10^{-4} \left(\frac{n}{10^{-5}} \right)^{1/2} \left(\frac{v_{\text{adv}}}{0.2c} \right) \text{Gauss}$$

and the observed value of B_{eq} in the hot spot is $\sim 1\,10^{-5}$ Gauss.

5.4. *Age of 3C236*

One of the most interesting questions regarding 3C236 concerns its age, T. There are two firm limits: (a) T must be larger than the light travel time from the nucleus to the SE lobe; (b) T must be smaller than the age of the universe. Thus we can set $10^{6.9} < T < 10^{10.3}$ yr. On this basis we reject the age of $\gtrsim 10^{11}$ yr deduced by S&W from their multiple plasmon model as improbable. The critical parameter in considering the age of 3C236 is the velocity at which the edges of the radio source advance outwards, v_{adv}. Statistics of radio sources in general suggest that $0.03c < v_{\text{adv}} < 0.1c$ (Begelman et al., 1984). Taking $v_{\text{adv}} \sim 0.05c$ gives $T \sim 10^{8.2}$ yr. Further information about the age of 3C236 is contained in the spectral index distribution along the very extended NW radio lobe.

The spectral behaviour of this NW lobe has been studied by Strom et al. (1981) and Saunders (1982). According to Strom et al. (1981) the spectral index α_{610}^{4825} appears to steepen from -0.6 at the leading edge to -1.2 at its trailing end where the 4825 MHz emission disappears in the noise. The spectral index may therefore steepen further in the direction of the galaxy. We here consider two possible evolutionary sequences for the NW lobe. First, the spectral behaviour described above is consistent with spectral aging, if we adopt the scenario that the diffuse lobe emission has been left behind in $\sim 10^{8}$ yr by a beam, advancing with velocity $\sim 0.1c$. Particle reacceleration may increase this time somewhat. The smooth appearance of the lobe is an argument in favour of its relaxed state, and identification as a radiotrail. As $B_{eq} \sim 1$ μG for the low brightness emission, static thermal pressure balance with the IGM is likely. In this scenario the large scale wiggle can be explained by either a hydrodynamic instability or precession of the advancing plasma flow. The inner ridge in the NW lobe (which shows a hot spot) could be regarded as a more recent event in the history of the radio galaxy: a new beam is entering the relaxed radio lobe. The presence of the ridge hot spot, NW of the associated galaxy, is not necessary in contradiction with the collimation similarities discussed earlier, since this inner ridge is not confined by the tenuous IGM, but instead by previously deposited NW lobe plasma.

A major problem with the first scenario however is the rather small age ($\sim 10^{8}$ yr), inferred for the NW lobe, considering its high internal mass; $\gtrsim 10^{10} M_{\odot}$ (S&W). A mass flow rate of $\sim 10^{2} M_{\odot}\,\text{y}^{-1}$ would be required, which seems rather high according to the current picture of radio source fuelling (Begelman et al., 1984). This mass problem would be overcome if the (marginal) depolarization as reported by S&W were to prove to be incorrect; the inferred thermal matter density, and consequently the total mass in the NW lobe would then be reduced.

The second scenario, which was proposed by S&W, is that the entire NW lobe emission has been built up by the energy deposit of many successive plasmons, like the inner ridge. Particle (re)accelaration throughout the lobe is required in this scenario, since the particle diffusion speeds are far too low to explain the spectral behaviour of the lobe (Strom et al., 1981). This scenario was discussed already in Sect. 5.3 and was considered less likely. We note further that in the case of a lower mass density (see above),

the demand for particle (re)acceleration for the evolution of the NW lobe in this second scenario would be less strong.

In any case, determination of the thermal mass density in the NW lobe will be essential for discriminating between the two scenarios, and this requires low frequency polarization mapping at high dynamic range with sufficient resolution.

In summary, the estimation of the age of 3C236 depends on which evolutionary sequence one adopts as the most probable and what interpretation is put on the spectral steepening which has been observed. The lower limit is set at 10^8 yr from consideration of the spectral steepening, assuming no additional particle injection, and component formation from a single event; the upper limit is the age of the universe, $10^{10.3}$ yr. Other evolutionary sequences leading to intermediate ages can also be imagined. We suggest adopting an age of $10^{9\pm1}$ y for 3C236.

In conclusion we emphasize that because of (a) its large size, and (b) the opportunity afforded to study the relation of structures on such a large range of scales, 3C236 is worthy of further investigation. Of particular interest will be high resolution optical images of the nucleus from the Space Telescope.

Acknowledgements. We thank Dr. T. J. Cornwell for supplying the MERLIN data and help with the 5 GHz VLBI observations. We thank Drs. S. C. Unwin, T. J. Pearson, J. Usowicz and F. Janssen, as well as the staffs of the CIT/JPL and MPIfR processors for help and advice in processing and reducing the VLBI data. We thank Dr. A. G. de Bruyn and Ir. J. F. Noordam for help with the redundancy observations and data reduction, Dr. V. Icke for discussions and Renée de Bruin and Maud Siksma for typing and retyping the manuscripts. PDB acknowledges support by the Netherlands Foundation for Astronomical Research (ASTRON). The WSRT is operated by the Netherlands Foundation for Radio Astronomy. Both foundations are financially supported by the Netherlands Organization for the Advancement of Pure Research (ZWO). PDB also acknowledges travel support from the Leids Kerkhoven-Bosscha Fonds.

References

Begelman, M.C., Blandford, R.D., Rees, M.J.: 1980, *Nature* **287**, 307
Begelman, M.C., Blandford, R.D., Rees, M.J.: 1984, *Rev. Mod. Phys.* **56**, 255
Biretta, J.A., Owen, F.N., Hardee, P.N.: 1983, *Astrophys. J. Letters* **274**, L 27
Blandford, R.D., Icke, V.: 1978, *Monthly Notices Roy. Astron. Soc.* **185**, 527
Blandford, R.D., Königl, A.: 1979, *Astrophys. J.* **232**, 34
Bridle, A.H., Famalont, F.B.: 1978, *Astron. J.* **83**, 704
Clark, B.G.: 1973, *Proc. IEEE* **61**, 1242
Cohen, M.H., Moffet, A.T., Ronney, J.D., Schilizzi, R.T., Shaffer, D.B., Kellermann, K.I., Purcell, G.H., Grove, G., Swenson Jr., G.W., Yen, J.L., Pauliny-Toth, I.I.K., Preuss, E., Witzel, A., Graham, D.: 1975, *Astrophys. J.* **201**, 249
Cornwell, T.J., Wilkinson, P.N.: 1981, *Monthly Notices Roy. Astron. Soc.* **196**, 1067
Davies, J.G., Anderson, B., Morrison, I.: 1980, *Nature* **288**, 64
Ferrari, A., Trussoni, E., Zaninetti, L.: 1983, *Astron. Astrophys.* **125**, 179
Fomalont, E.B., Miley, G.K.: 1975, *Nature* **257**, 99
Fomalont, F.B., Miley, G.K., Bridle, A.H.: 1979, *Astron. Astrophys.* **76**, 106
Fomalont, E.B., Bridle, A.H., Miley, G.K.: 1982, in *Extragalactic Radio Sources, Proc.* IAU *Symp.* **97**, eds. Heeschen, Wade, Reidel, Dordrecht, p. 173
Fomalont, E.B., Palimaka, J.J., Bridle, A.H.: 1980, *Astron. J.* **85**, 981
Heckman, T.M., Miley, G.K., van Breugel, W.J.M., Butcher, H.R.: 1981, *Astrophys. J.* **247**, 403
Lonsdale, C.J., Barthel, P.D.: 1985 (in preparation)
Miley, G.K., Osterbrock, D.E.: 1979, *Publ. Astron. Soc. Pacific* **91**, 257
Noordam, J.E., de Bruyn, A.G.: 1982, *Nature* **299**, 597
Osterbrock, D.E.: 1984, *Quart. J. Roy. Astron. Soc.* **25**, 1
Owen, F.N., Hardee, P.E., Bignell, R.C.: 1980, *Astrophys. J. Letters* **239**, L 11
Preuss, E., Pauliny-Toth, I.I.K., Witzel, A., Kellermann, K.I., Shaffer, D.B.: 1977, *Astron. Astrophys.* **54**, 297
Readhead, A.C.S.: 1980, in *Objects of High Redshift, Proc.* IAU *Symp.* **92**, eds. Abell, Peebles, Reidel, Dordrecht, p. 165
Rees, M.J.: 1978, *Nature* **275**, 516
Rees, M.J.: 1979, *Monthly Notices Roy. Astron. Soc.* **184**, 61 P
Saikia, D.J.: 1981, *Monthly Notices Roy. Astron. Soc.* **197**, 1097
Sandage, A.: 1967, *Astrophys. J. Letters* **150**, L 145
Saunders, R.: 1982, *Observatory* **102**, 128
Schilizzi, R.T., de Bruyn, A.G.: 1983, *Nature* **303**, 26
Schilizzi, R.T., Miley, G.K., van Ardenne, A., Baud, B., Bååth, L.B., Rönnäng, B.O., Pauliny-Toth, I.I.K.: 1979, *Astron. Astrophys.* **77**, 1
Schilizzi, R.T., Miley, G.K., Janssen, F.L.J., Wilkinson, P.N., Cornwell, T.J., Fomalont, E.B.: 1981, in *Optical Jets in Galaxies*, Proc. ESO/ESA Workshop, p. 107
Strom, R.G., Willis, A.G.: 1980, *Astron. Astrophys.* **85**, 36 (S&W)
Strom, R.G., Baker, J.R., Willis, A.G.: 1981, *Astron. Astrophys.* **100**, 220
Trussoni, E., Ferrari, A., Zaninetti, L.: 1983, in *Astrophysical Jets, Proc. Torino Workshop*, Reidel, Dordrecht, p. 281
Van Breugel, W., Miley, G., Heckman, T.: 1984, *Astron. J.* **89**, 5
Wilkinson, P.N.: 1972, *Monthly Notices Roy. Astron. Soc.* **160**, 305
Willis, A.G., Strom, R.G., Wilson, A.S.: 1974, *Nature* **250**, 625
Wyndham, J.D.: 1966, *Astrophys. J.* **144**, 459